OBSERVATIONS OF FLUID ACCELERATIONS WITHIN INDIVIDUAL SWASH EVENTS

Diane Foster[1], Emily Carlson[2], Daniel Conley[3], Jack Puleo[4]

Abstract

A proto-type laboratory experiment examining the barrier dynamics over a sandy beach with a landward lagoon system was conducted in the Spring and Summer of 2012 during the collaborative BARDEX II experiment. This investigation focuses on the near bed hydrodynamic structure within 3 cm of the bed in the outer swash zone. Horizontal velocity profile observations show significant variability over the phase of a wave. These results highlight the opportunity for high-resolution velocity profile observations in the swash zone. The observations show statistically robust temporal means as a function of wave phase that could be used to evaluate numerical simulations of the flow field and sediment transport.

Key words: swash zone, sediment transport, pressure gradients, BARDEX II

1. Introduction

The complex dynamics of water surface elevations and fluid motions in the swash zone leading to sediment transport can vary appreciably within a single swash event (Puleo et al., 2000; Turner et al., 2008; and Puleo et al, 2012). Based on the early energetics-based sediment transport models of Bagnold (1966), the primary mechanism of sediment transport in the swash has been assumed to be the bed shear stress (for a review, please see Elfrink and Baldock, 2002; Puleo et al., 2012). The shear stress can change significantly over individual runup events and can result in either new onshore or offshore sediment transport. According to Sleath (1999), the horizontal pressure gradient can apply an additional force applied to a sediment bed that can work to further stabilize or destabilize the sediment bed (Foster et al., 2006a). In some sediment transport formulations, this pressure gradient contribution is attributed to a fluid acceleration effect (Puleo et al., 2003, Drake and Calantoni, 2001). The goal of this effort is to examine the fluid accelerations within individual swash events.

Observations of the dynamics leading to a morphologic adjustment require the spatial and temporal resolution of the velocity, acceleration, and shear stress fields. Observations of these parameters are complicated, as the sampling region consists of three-phase fluid: suspended sediment, fluid, and entrapped air. These complications result in significant challenges in observational sampling of both the flow and morphology. In this effort, the local fluctuations of velocity, acceleration, and bed elevation within particular swash events will be examined with new high-resolution observations within the outer swash zone.

2. Observations

The goal of the BARrier Dynamics EXperiment (BARDEX II) was to examine the complex dynamics within a coastal barrier system and develop an increased understanding of sediment transport processes on

[1]Dept. of Mech. Engin., W101 Kingsbury Hall, Univ. of New Hampshire, Durham, NH, 03824, diane.foster@unh.edu.
[2]Center for Ocean Engin., Jere. A. Chase Ocean Engin. Laboratory, Univ. of New Hampshire, Durham, NH, 03824, em144@wildcats.unh.edu.
[3]School of Marine Science and Engin., Univ. of Plymouth, Room 121, Reynolds, Drake Circus, Plymouth, Devon, PL4 8AA, daniel.conley@plymouth.ac.uk.
[4]Dept. of Civil and Envir. Engin., University of Delaware, Newark, DE, 19716, jpuleo@udel.edu.

sandy beaches (Masselink et al, 2012). The observations were obtained in the Delta Flume in Vollenhove, Netherlands during the spring and summer of 2012. The project was hosted by Deltares, and is a collaboration of twenty-five researchers from nine universities from around the world. The Delta flume is 5 m wide, 240 m long, and 7 m deep, and contained 1,400m^3 of medium grained sand (d_{50} = 0.4 mm). Prior to the observations, the bathymetry was shaped and compacted into a beach and lagoon system.

The observations used in this effort were located at the outermost swash station (see Masselink et al., 2013). A Nortek Vectrino II Doppler profiler sampled three components of velocity at 1 mm range bins over a 31 mm range at 100 Hz. The highest and the lowest sampling locations are 4 cm and 7 cm from the sensor head (Figure 1). The lowest location (7 cm from the sensor head) is herein defined as the reference location (z=0). The bed elevation varies with time and may be either above or below the z=0 reference location. The uppermost location (4 cm from the sensor head) is the elevation farthest from the bed and will be used as an approximate free stream location. In between individual wave simulations, the morphology local to each instrument was recorded. Ancillary data was provided by nearby pressure sensors and electromagnetic current meters (not presented here).

In the data analyzed here, a broad banded wave spectrum was created by the active wave-absorbing paddle with a significant wave height of 0.8 m and a peak period of 8 s. This particular simulation was 3-hours long, allowing for an examination of the larger scale morphologic response of the nearshore system. This effort will focus on a single 10-minute record within the 3-hour run when the bed remained relatively uniform. The instrument was located in the outer swash but within the runup tongue.

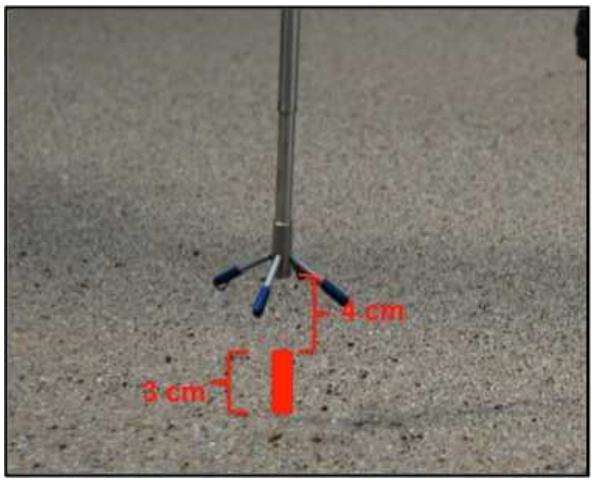

Figure 1. A snapshot of the Vectrino II over a dry sediment bed. The 3 cm profiling range is located below the 4 cm blanking distance.

Data at every range bin were retained when the instantaneous correlation value (averaged over the four beams) of greater than 70%. One of the following three conditions could result in poor correlations: 1) the sensor is not submerged; 2) the void fraction is high; and 3) the 1 mm volume has a high sediment concentration. The water level exceeded the sensor head and the acoustic correlations exceeded the prescribed threshold roughly 30% of the 10-minute window.

The internal bed finding algorithm for the sensor was sampled at a frequency of 1 Hz. For the dynamic nature of the swash zone, this was not high enough to capture variability within individual swash events. The local bed elevation was determined with the sensor signal to noise ratio (SNR) averaged over the 4 beams for regions when the data was deemed good. A lowpass filter with a 10-point Butterworth window was applied to the SNR time series to remove spurious data. The bed elevation was approximated at the location with the highest low pass filtered SNR value within the sampling range. For these observations, the SNR threshold was iteratively determined to be 57.5.

3. Results

Figure 2 shows a sample 60-second time series of the velocity and local acceleration at three elevations. The acceleration is estimated from the slope by fitting a straight line to overlapping 1-second windows (100 points). 1-second windows that have more than 50% of bad data were rejected. With the exception of the swash event surrounding 90 s, the reference elevation (z=0 cm) over this 60-second record is at or near the bed elevation as indicated by the mostly zero velocity and acceleration amplitudes.

A closer examination of the horizontal velocity and acceleration profiles over three swash events between 100 and 130 seconds is shown in Figure 3. The velocity field within each event shows significant temporal variability, but less variability with elevation suggesting a thin well defined boundary layer. Consistent with previous swash observations, the acceleration shows less temporal variability in time. These observations are also consistent with the numerical simulations of Puleo et al. (2007) who showed swash accelerations to be positive only at the very beginning of the swash event, but are offshore directed through the remainder of the swash event. The magnitude of the acceleration can exceed 1.0 m/s^2, but is more typically between -0.5 m/s^2 and 0. Positive accelerations (accelerating onshore flow or decelerating backwash flow) occur rarely. Bed elevations estimates from the internal manufacturer algorithm and from

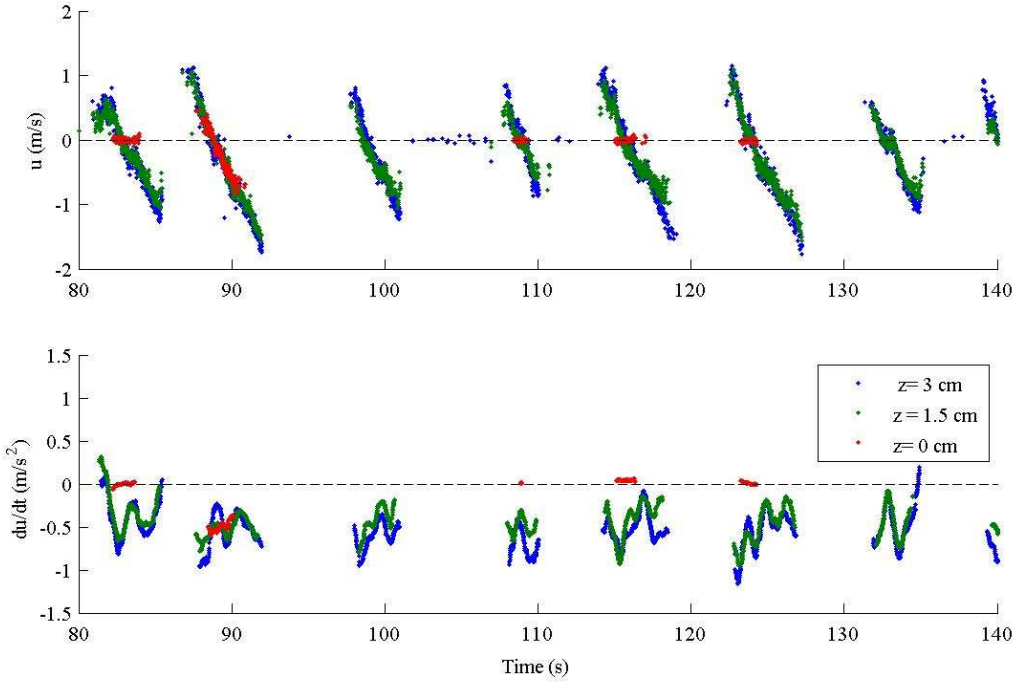

the SNR method described above are generally coincident with locations where the velocity and acceleration approaches zero.

Figure 2. An example 60-second time series of (upper) horizontal velocity and (lower) local acceleration at z=0, 1.5, and 3 cm from reference. Onshore directed flow is defined with positive velocities.

The likelihood of pressure gradient induced sediment motion can be evaluated with the Sleath parameter, *S*, given by

$$S = \frac{Du_\infty / Dt}{(s-1)g} \qquad (1)$$

where s is the specific gravity (=2.65 for quartz sediment), g is the gravitational acceleration (=9.81 m/s^2), and u_∞ is the free stream velocity (Sleath, 1999). It should be noted that this formulation was based on

force balance over a slab of sediment on a non-sloping bed. Moreover, the formulation assumes that the horizontal pressure gradient can be approximated with the acceleration, in this case the local acceleration as measured at the uppermost location (z=3 cm). According to the wave bottom boundary layer surf zone field observations of Foster et al. (2006b), the pressure gradient induced incipient motion can occur when S > 0.08. For the observations considered in this effort the critical threshold for incipient motion would be exceeded when the acceleration magnitude exceeds 1.3 m/s^2. In the last two swash events shown in Figure 3, the peak acceleration magnitudes approach this critical threshold and may be followed by either large signal attenuation possibly due to sediment mobilization or bed accretion, as is evident by the rise in the apparent bed elevation.

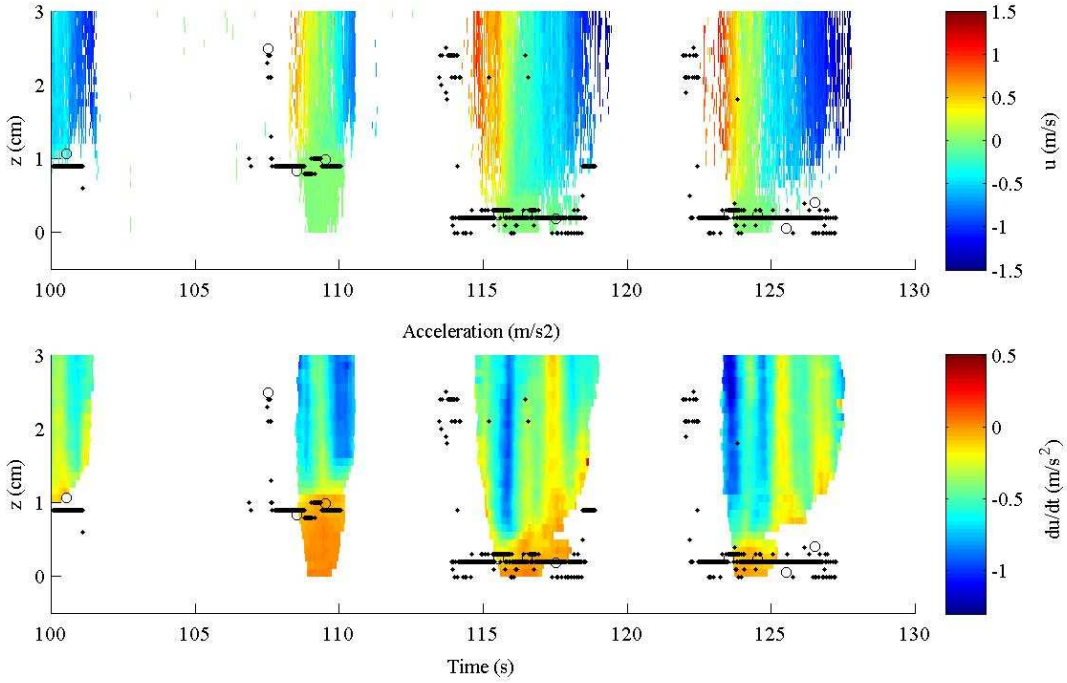

Figure 3. An example 30-second time series of (upper) horizontal velocity and (lower) local acceleration as a function of elevation. z=0 represents the reference elevation. Onshore-directed flow is defined with positive velocities. The open circles represent the Vectrino II estimates of the bed elevation and the black dots represent the instantaneous bed elevations.

Robust statistical characterization of swash zone hydrodynamics are limited by intermittent wetting and drying of the bed, variation in bed elevation, as well as high levels of noise. In the case of regular waves commonly assumed in laboratory observations, an ensemble averaging technique can be used to examine the dynamics relative to wave phase (i.e., 0 ^{o} to 360^o). Because the swash zone in the field (and in this laboratory study) is composed of a random wave field, we follow Foster et al. (2006a) and define an analogous random wave phase as a function of the instantaneous velocity and acceleration at the uppermost sampling location (z=3 cm above the lowermost reference sampling location). This phase-space averaging (PSA) technique allows for the evaluation of the magnitude and evolution of physical quantities, such as velocity and acceleration as a function of water depth over the phase space. Each quantity of interest is averaged over the comparable reference wave velocities, u(z=3 cm,t), and local accelerations, du/dt(z=3 cm,t). Providing there are enough occurrences at an individual velocity-acceleration bin, it is possible to obtain statistically robust averages as a function of wave phase.

The sample mean of the quantity in each bin is computed, producing a 'phase-space' average. If the waves were purely sinusoidal with a single amplitude, the PSA would lead to an ellipse with a vertical (acceleration) to horizontal (velocity) ratio of the angular frequency. For minimal statistical stability, we require that at least 10 realizations be present in each observation. For all figures, the eight velocity bins

are centered on -1.80, -1.4, -1.0, -0.6, -0.2 0.2, 0.6 1.0 m/s with a 0.4 m/s window about each bin. Similarly, the six acceleration bins are centered on -1.25, -0.75, 0.25, 0.25, 0.75, 1.25 m/s^2 with a 0.5 m/s^2 window about each bin. The flow moves in a clockwise direction around the figure. Because the Doppler correlations for each sampling location may vary, not all elevations will contain the same number of estimates. In describing the following results, we define uprush as positive velocities and downwash as negative velocities. Strengthening flows have an increasing velocity magnitude and similarly weakening flows have a decreasing velocity magnitude.

Figure 4 shows the PSA of the number of occurrences for each reference velocity and acceleration bin. Positive accelerations often have water depths that do not reach the sensor head (at least 7 cm from the bed), and consequently have fewer realizations. The PSA shows that the velocity at the reference location ranges -1.75 to 1 m/s, with the highest density of observation in the offshore directed strengthening flow quadrant ($u < 0$ m/s and $du/dt < 0$ m/s^2). The dominant acceleration of 0.5 m/s^2 is consistent with the slope of the velocity records shown in Figure 2. The shorter duration uprush periods have a slightly larger range of accelerations. This is particularly true for the positive accelerations during the uprush.

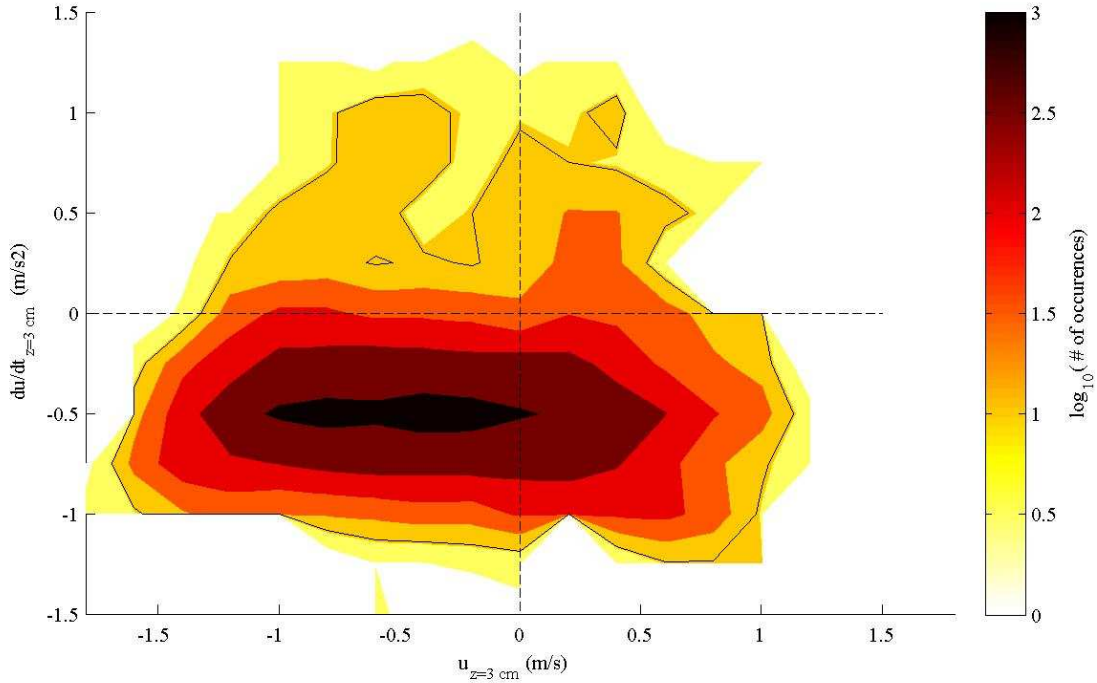

Figure 4. The phase space average distribution of the number of occurrences with each horizontal velocity and acceleration bin over a 10-minute realization. The colors indicate the $\log_{10}$ of the number of occurrences.

Figure 5 shows the PSA for the horizontal velocity field versus the elevation. Statistical variability is shown by horizontal bars representing +/- 1 standard deviation from the mean at every location. Onshore-directed uprush ($u > 0$ m/s) mean velocities generally have lower variability and would suggest consistent hydrodynamic response to the bore propagating up the beach. During the relatively short duration of the weakening uprush flow phase ($u > 0$ m/s and $du/dt < 0$ m/s^2), the velocity profiles show a reasonably well developed boundary layer with thicknesses of roughly 2 cm. During this flow phase, the velocity profiles show velocities of nearly zero at the reference elevation and suggest a no-slip condition would be valid.

During the relatively longer duration of the strengthening downwash flow phase ($u < 0$ m/s and $du/dt < 0$ m/s^2), the boundary layer grows and reaches or exceeds the upper observable elevation ($z = 3$ cm). The longer duration of the downrush allows for increased boundary layer development and would be expected to produce larger boundary layer thicknesses. It is of interest to note that for velocities with magnitudes greater than 0.4 m/s ($u(z=3\text{ cm}) < -0.4$ m/s) and accelerations with magnitudes greater than 0.5 m/s^2 ($du/dt(z=3\text{ cm}) < -0.5$ m/s^2), the velocity near the bed, approaches but does not generally reach zero.

There are two possible explanations: 1) there is a temporary bed accretion as a mass of sediment that moves past the sensor or 2) and more likely, the sensor signal strength is attenuated due to suspended particles in the nearbed region. A mobile sheet flow layer would result in significant acoustic attenuation within the mobile sediment layer. Either explanation suggests significant sediment motion during this flow phase. The last two swash events in Figure 3 are particularly good examples of this phenomenon. In both cases, following flow reversal, the near bed acoustic correlations result in inaccurate velocity estimates. These mobilizations occur during the largest accelerations (and pressure gradients) and well before the peak shear stress would occur. Consequently, the sediment motion during these larger events may be significantly affected by the horizontal pressure gradient.

Figure 6 shows the PSA for the acceleration field versus the elevation. Statistical variability is shown by horizontal bars representing +/- 1 standard deviation from the mean at every location. As with the velocity field, the accelerations generally approach zero very near the reference elevation. Please note that the reference elevation is approximately at the bed elevation for the two larger swash events shown in Figure 3. A decrease in the local inertia is consistent with wave bottom boundary layer theory, which suggests that at the bed, the inertia is zero. If the wave bottom boundary layer equation is valid during the moderate conditions as these observations suggest, then the vertical decay of the local acceleration may provide an alternative method for estimating the shear stress gradient with

$$\frac{\partial T}{\partial z} = \frac{\partial u}{\partial t} - \frac{\partial u_\infty}{\partial t} \qquad (2)$$

where T is the shear stress. Integrating the acceleration deficit over the sampling volume could allow for an approximation of the bottom shear stress. An exception to the zero inertia in the very near bed region is during large accelerations ($du/dt(z=3\text{ cm}, t) < -1.0\text{ m/s}^2$). When the magnitude exceeds 1 m/s^2, the accelerations only slightly decrease through the sampling volume and are suggestive of the pressure gradient induced motion.

4. Summary

A proto-type laboratory experiment examining the barrier dynamics over a sandy beach with a landward lagoon system was conducted in the spring and summer of 2012 during the collaborative BARDEX II experiment. This investigation focussed on the near bed hydrodynamic structure within 3 cm of the bed in the outer swash zone. Horizontal velocity profile observations show significant variability over the phase of a wave. The horizontal velocity approaches zero at or near the reference elevation and during most flow phases would be in general support of a no-slip bottom boundary condition. Moreover, through most flow phases, the local inertia approaches zero in the very near bed region. These findings would suggest that during moderate swash events, the wave bottom boundary layer may be valid and the shear stress can be estimated by integrating the acceleration deficit.

During more extreme swash events when the velocity and acceleration magnitudes are large (particularly during the strengthening phase of the downwash), the dynamics and sediment motion may be affected by the pressure gradients. In these situations, the local inertia remains large near the bed and the velocity profile does not reach a no-slip zero velocity condition. Ancillary support for significant sediment transport during these more extreme conditions is provided by the loss of good data in the near bed region of the profile that could result from significant signal attenuation due to suspended sediment.

These results highlight the opportunity for high-resolution velocity profile observations in the swash zone. The observations show statistically robust temporal means as a function of wave phase that could be used to evaluate numerical simulations of the flow field and sediment transport.

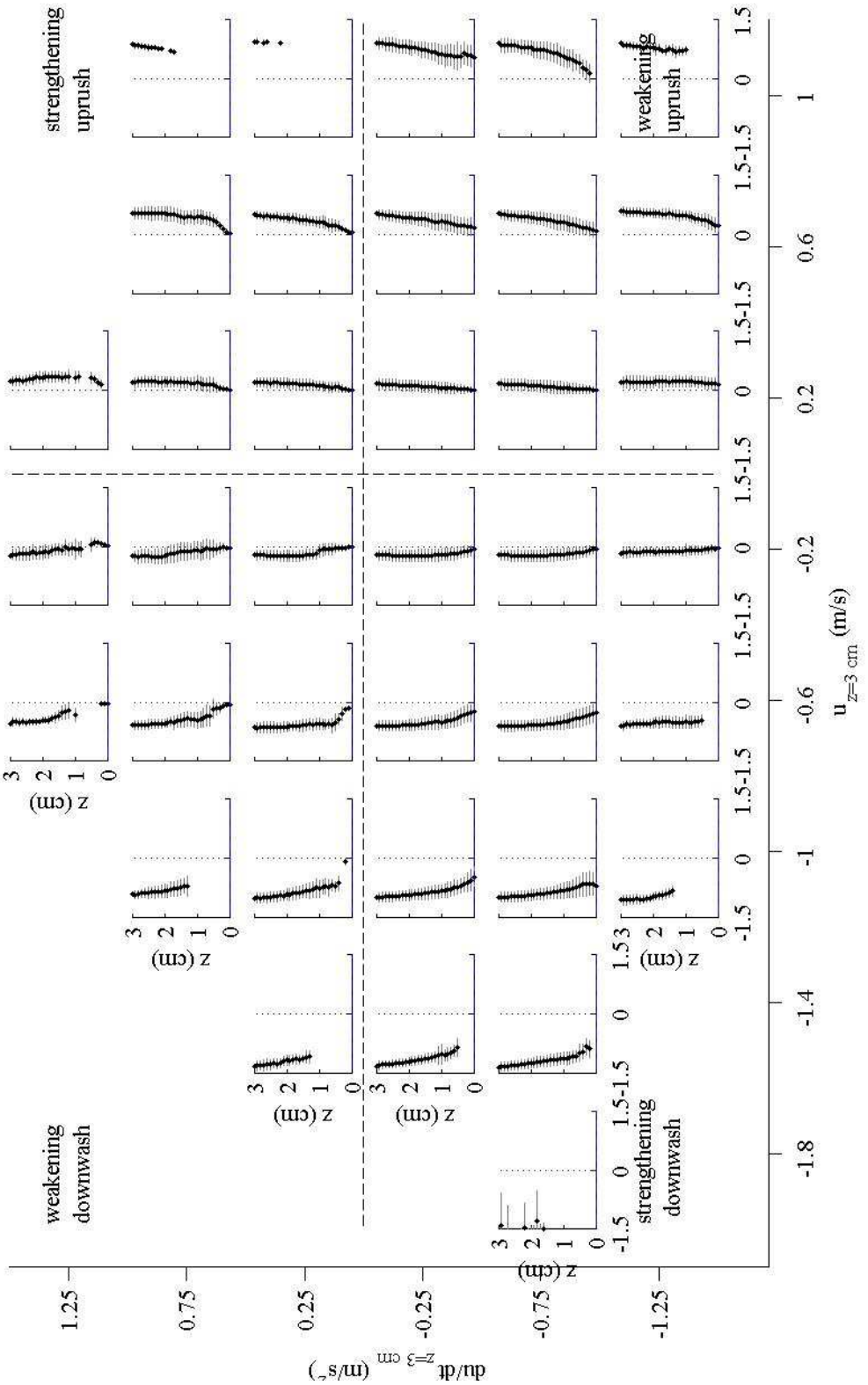

Figure 5. The phase space average distribution of velocity versus elevation over a 10-minute time series. The vertical axis of each independent plot is elevation relative to the reference location, ranging from 0 to 3 cm, and the horizontal axis is horizontal velocity, ranging from -1.5 m/s to 1.5 m/s. The gray horizontal lines show +/- 1 standard deviation about the mean estimate (black dots).

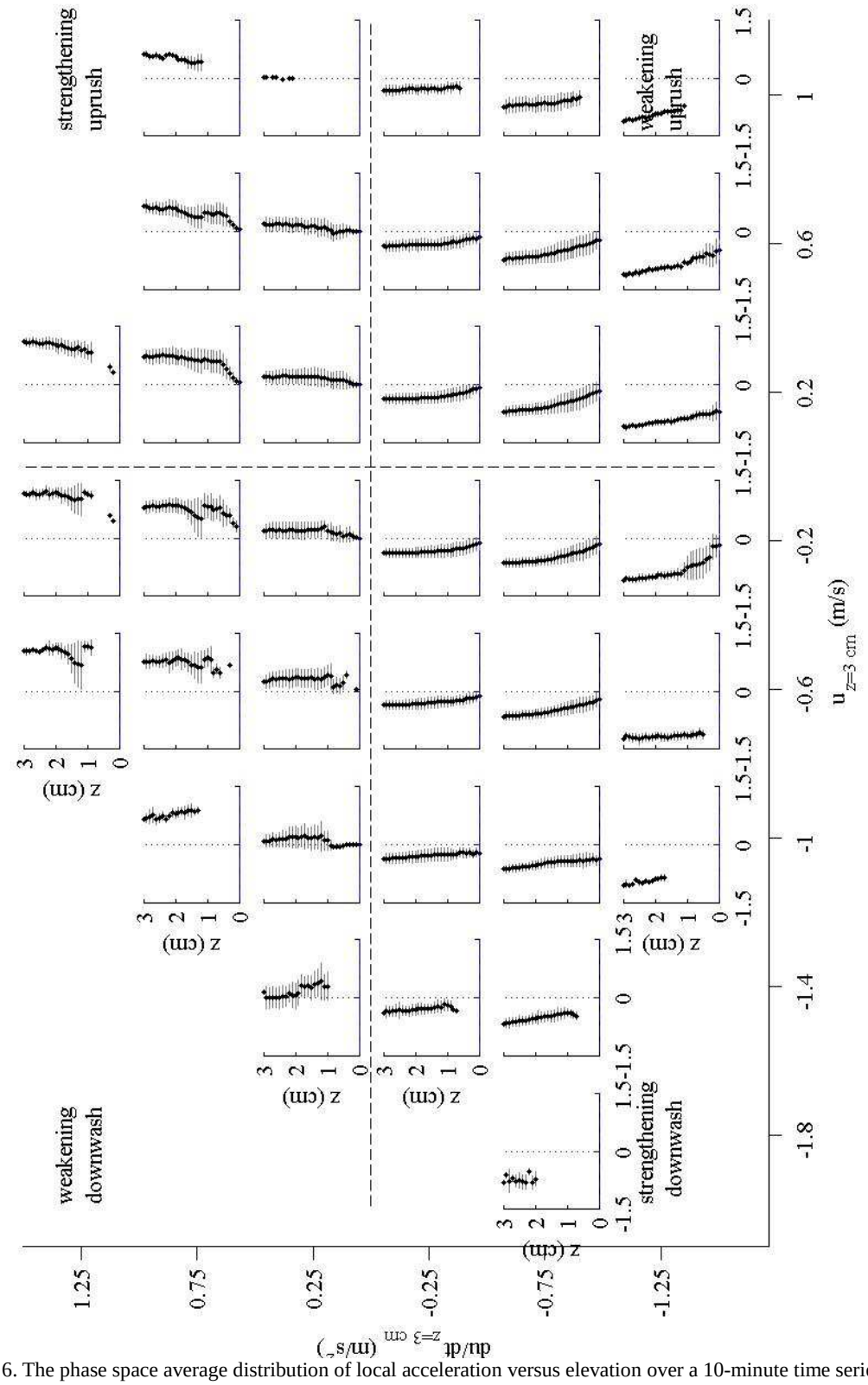

Figure 6. The phase space average distribution of local acceleration versus elevation over a 10-minute time series. The vertical axis of each independent plot is elevation relative to the reference location, ranging from 0 to 3 cm, and the horizontal axis is horizontal velocity, ranging from -1.5 m/s to 1.5 m/s. The gray horizontal lines show +/- 1 standard deviation about the mean estimate (black dots).

5. Acknowledgements

This effort has been supported by the National Science Foundation, NEESR and CBET programs. The work described in this publication was supported by the European Community's 7th Framework Programme through the grant to the budget of the Integrating Activity HYDRALAB IV, contract no. 261520. The authors would like to specifically acknowledge the field efforts of Thijs Lanckriet and Berkley Sadana, and the rest of the Bardex II crew.

6. References

Bagnold, R.A., 1966. An approach to the sediment transport problem from general physics, Professional Paper Rep, 42 2-I. U.S. Geological Survey, Washington, DC. 37 pp.

Barnes, M.P., O'Donoghue, T.O., Alsina, J.M., Baldock, T.E., 2009. Direct bed shear stress measurements in bore-drive n swash. Coastal Engineering (56), 853–867.

Drake, T. G., & Calantoni, J., 2001. Discrete particle model for sheet flow sediment transport in the nearshore. *Journal of Geophysical Research: Oceans (1978–2012)*, *106*(C9), 19859-19868.

Elfrink, B., Baldock, T., 2002. Hydrodynamics and sediment transport in the swash zone: a review and perspectives. J. Coastal Eng. 45, 149-167.

Foster, D., Beach, R., and Holman, R., 2006a. Turbulence Observations of the Nearshore Wave Bottom Boundary Layer, *Journal of Geophysical Research*, 111(C4), C04011, 1-11.

Foster, D. L., Bowen, A. J., Holman, R. A., & Natoo, P., 2006b. Field evidence of pressure gradient induced incipient motion. *Journal of Geophysical Research: Oceans (1978–2012)*, *111*(C5).

Masselink, G., Puleo, J.A., 2006. Swash-zone morphodynamics. Continental Shelf Research 26, 661–680.

Masselink, G, Turner, I.L., Conley, D.C., Ruessink, B.G., Matias, A., Thompson, C., Castelle, B. and Wolters, G., 2013. BARDEX II: Bringing the beach to the laboratory – again! *In:* Conley, D.C., Masselink, G., Russell, P.E. and O'Ha re, T.J. (eds.), *Proceedings 12th International Coastal Symposium*, Journal of Coastal Research, Special Issue, No. 6 5. Plymouth, England, ISSN 0749-0208.

Puleo, J.A., Holland, K.T., Plant, N., Slinn, D.N., Hanes, D.M., 2003. Fluid acceleration effects on suspended sediment transport in the swash zone. Journal of Geophysical Research 108, 3350, http://dx.doi.org/10.1029/2003JC001943.

Puleo, J. A., A. Farhadzadeh, and N. Kobayashi (2007), Numerical simulation of swash zone fluid accelerations, *J. Geo phys. Res.*, *112*, *C07007*, *doi:10.1029/2006JC004084*.

Puleo, J. A., Lanckriet, T., & Wang, P., 2012. Near bed cross-shore velocity profiles, bed shear stress and friction on the foreshore of a microtidal beach. *Coastal Engineering*, *68*, 6-16.

Sleath, J. F. A., 1999. Conditions for plug formation in oscillatory flow. *Continental Shelf Research*, *19*(13), 1643-1664.

Turner, I., Russell, P., Butt, T., 2008. Measurement of wave-by-wave bed-levels in the swash zone. Coastal Engineering 55, 1237–1242.